Oecologia
https://doi.org/10.1007/s00442-022-05226-4

HIGHLIGHTED STUDENT RESEARCH

Light dependence in the phototrophy–phagotrophy balance of constitutive and non-constitutive mixotrophic protists

Luca Schenone[1] · **Esteban Balseiro**[1] · **Beatriz Modenutti**[1]

Received: 30 November 2021 / Accepted: 20 July 2022

Abstract

Mixotrophic protists display contrasting nutritional strategies and are key groups connecting planktonic food webs. They comprise constitutive mixotrophs (CMs) that have an innate photosynthetic ability and non-constitutive mixotrophs (NCMs) that acquire it from their prey. We modelled phototrophy and phagotrophy of two mixotrophic protists as a function of irradiance and prey abundance. We hypothesised that differences in their physiology (constitutive versus non-constitutive mixotrophy) can result in different responses to light gradients. We fitted the models with primary production and bacterivory data from laboratory and field experiments with the nanoflagellate *Chrysochromulina parva* (CM) and the ciliate *Ophrydium naumanni* (NCM) from north Andean Patagonian lakes. We found a non-monotonic response of phototrophy and phagotrophy to irradiance in both mixotrophs, which was successfully represented by our models. Maximum values for phototrophy and phagotrophy were found at intermediate irradiance coinciding with the light at the deep chlorophyll maxima in these lakes. At lower and higher irradiances, we found a decoupling between phototrophy and phagotrophy in the NCM while these functions were more coupled in the CM. Our modelling approach revealed the difference between both mixotrophic functional types on the balance between their nutritional strategies under different light scenarios. Thus, our proposed models can be applied to account how changing environmental conditions affect both primary and secondary production within the planktonic microbial food web.

Keywords Microbial loop · Modelling · Irradiance · Primary production · Bacterivory

Communicated by Donald DeAngelis.

Mixotrophy, a feeding strategy using both autotrophic and heterotrophic carbon sources, is widely distributed in microscopic plankton but rarely included in ecological models. We have developed a model for the balance between the rates of photosynthesis (phototrophy) and prey ingestion (phagotrophy) in two types of mixotrophic protists - constitutive and non-constitutive. We validate the model using experimental data from field and laboratory research on two protist species that are widely distributed in high-mountain lakes of Patagonia. Our modelling approach clearly identified how a constitutive and a non-constitutive mixotrophic protist species balances their nutritional modes under a wide irradiance range.

✉ Luca Schenone
lucaschenone@comahue-conicet.gob.ar

Esteban Balseiro
ebalseiro@comahue-conicet.gob.ar

Beatriz Modenutti
bmodenutti@comahue-conicet.gob.ar

[1] Laboratorio de Limnología, INIBIOMA-CONICET, Universidad Nacional del Comahue. Quintral 1250, 8400 San Carlos de Bariloche, Río Negro, Argentina

Introduction

Mixotrophy is a nutrition mode that combines both phototrophy and heterotrophy through photosynthesis and organic carbon uptake. Although mixotrophy can include other forms of nutrition (Jones 1997), in this work we will consider protists that obtain energy and nutrients by phototrophic autotrophy (using light) and phagotrophic heterotrophy (by particle uptake). The increase in microbial plankton research has revealed that mixotrophic protists are very common in aquatic environments (Jones 2000; Stoecker 1998) and a major component in many planktonic food webs (Flynn et al. 2019). The recognition of the ecological importance of the microbial loop in plankton trophic dynamics (Azam et al. 1983) and the ability to utilise multiple ways of energy and nutrient acquisition, place mixotrophs as a key group within the planktonic food web (Ward and Follows 2016) merging the traditional dichotomy of autotrophic phytoplankton and heterotrophic microzooplankton (Mitra et al. 2016). In this sense, mixotrophic protists may represent

Published online: 13 August 2022

a considerable fraction of the primary producers and bacterial grazers (Zubkov and Tarran 2008) constituting a key link between the microbial loop and higher trophic levels (Mitra et al. 2014; Ptacnik et al. 2004).

In high light–nutrient limited systems, bacterivory by mixotrophs is a particularly important predator–prey interaction (Modenutti and Balseiro 2002; Unrein et al. 2014; Yvon-Durocher et al. 2017). In these systems, mixotrophs have a physiological advantage over strict autotrophs because bacterivory provides essential nutrients to compensate for carbon fixation by phototrophy (Mitra et al. 2016). Phototrophic protists including strict phototrophs and mixotrophs, compete for nutrients with picoplankton that outcompete the formers due to a higher surface-to-volume ratio (Danger et al. 2007). In this context, mixotrophy represents an ecological advantage for protists by eating their competitor (Fischer et al. 2017; Nygaard and Tobiesen 1993). The effect of light on phototrophy of mixotrophs is well documented and has been assessed by both experimental and modelling approaches (Berge et al. 2017; Edwards 2019; Fischer et al. 2017; Waibel et al. 2019). On the other hand, phagotrophy is directly affected by prey availability and modulated by changes in dissolved nutrients and light (Edwards 2019; Hansson et al. 2019; Maselli et al. 2022). Although the effect of irradiance on the bacterivory of different mixotrophic species has been assessed with both field and laboratory experiments (Balseiro et al. 2004; Ptacnik et al. 2004; Waibel et al. 2019), mechanistic models involving a wide range of irradiance are still scarce. Recently, the non-monotonic Platt equation was proposed to model mixotrophic nanoflagellates (MNF) clearance rate in mountain lakes with a wide irradiance range, showing the high potential of Platt formulations to represent quantitatively how bacterivory is modulated by intermediate and high irradiances (Schenone et al. 2020).

Mixotrophs are extremely diverse and only by assigning their diversity metabolisms it will be possible to understand how they impact ecological dynamics and nutrient fluxes. Particularly, MNF were traditionally considered as 'phagotrophic phytoplankton', with most groups being primarily phototrophic but that benefit from phagotrophy according to light availability (Jones 1997). On the other hand, mixotrophic ciliates were traditionally named as 'photosynthetic protozoa' (primarily phagotrophic) in which phototrophy supplements C for nutrition (Stoecker et al. 2009). Recently, Mitra et al. (2016) categorised mixotrophs in two main functional groups: constitutive mixotrophs (CMs) that have an innate photosynthetic ability (i.e. have their photosystems) such as the MNF, and non-constitutive mixotrophs (NCMs) that acquire the photosystems from their prey, such as larger dinoflagellates and ciliates. CMs are more flexible to switch between nutritional strategies depending on the environmental conditions (Berge et al. 2017; Laybourn-Parry et al. 2005), while NCMs rely on the prey from which phototrophy is acquired (Leles et al. 2021). These approaches indicate that addressing mixotrophic diversity and how environmental factors affect their phototrophy–phagotrophy balance, can have an important impact on microbial food web dynamics.

Here, we modelled phototrophy and phagotrophy of two mixotrophic species in order to test the hypothesis that differences in their physiology (constitutive versus non-constitutive mixotrophy) can result in different responses to light gradients. By using a Bayesian modelling approach, we fitted the models with previous published literature on primary production and bacterivory data obtained from laboratory and field experiments with the nanoflagellate *Chrysochromulina parva* (CM) and the ciliate *Ophrydium naumanni* (NCM) of north Patagonian Andean lakes. These lakes are very transparent and thus represent an excellent scenario to study both phototrophy and phagotrophy in a wide irradiance range. Due to differences in physiology and lineage between both mixotrophs, we expect that the balance between phototrophy and phagotrophy will be more coupled in the flagellate than in the ciliate as light intensity shifts from the optimal range.

Materials and methods

Data compilation

To test our hypothesis, we compiled data from published literature on laboratory and field experiments performed in north Patagonian Andean lakes (Balseiro et al. 2004; Callieri et al. 2007; Modenutti and Balseiro 2020; Modenutti et al. 2004; Schenone et al. 2020) (Table 1). Glacial lakes of the North Andean Patagonian region (41°S, Argentina) are oligotrophic (Chlorophyll a < 1 µg L^{-1}, Total phosphorus < 5 µg L^{-1}) and very transparent (attenuation coefficient of photosynthetically active radiation [PAR, 400–700 nm] K_d: 0.1–0.2 m^{-1}). The high light penetration implies a wide euphotic zone and the development of deep chlorophyll maxima (DCM) where the highest photosynthetic efficiency and phytoplankton (mixotrophs and autotrophic picoplankton) abundance occur at depths near the 1% of surface PAR (Callieri et al. 2007; Modenutti et al. 2013). In all cases, phototrophy was estimated from primary production measurements using the ^{14}C technique (Nielsen 1952) in field experiments and then filtration to obtain MNF > 2 µm or in the laboratory with the exposure of a known number of *O. naumanni* (NCM). Phagotrophy was estimated from bacterivory experiments using the fluorescently labelled bacteria (FLB) technique and then counting under epifluorescence microscopy that allows the identification of the prey inside the studied protists (CM or NCM) (Sherr et al. 1987). The number of prey ingested was transformed to pg C assuming

Table 1 Compilation of the *Chrysochromulina parva* (CM) and *Ophrydium naumanni* (NCM) phototrophy and phagotrophy field and laboratory experiments used for model fitting.

Mixotrophic species	Experiment type	Function	Method	Lake	*I* (N° levels tested)	*N*	Replicates	Reference
C. parva	Field	Phototrophy	^{14}C	N. Huapi Moreno Espejo Correntoso Mascardi	17–1750 (8)	–	3	Callieri et al. (2007)
C. parva	Field	Phagotrophy	FLB	Rivadavia Moreno Mascardi Cántaros Verde	0–1250 (8)	6.7–20.1	3	Balseiro et al. (2004); Schenone et al. (2020)
O. naumanni	Laboratory	Phototrophy	^{14}C	Moreno	5–730 (8)	–	4	Modenutti et al. (2004)
O. naumanni	Field, laboratory	Phagotrophy	FLB	Rivadavia Moreno	0–600 (10)	13.8–28.6	3–4	Balseiro et al. (2004); Modenutti and Balseiro (2020)

^{14}C ^{14}C technique, *FLB* Fluorescently labelled bacteria, *I* irradiance range (µmol photon m^{-2} s^{-1}), *N* prey abundance range (ng mL^{-1})

15 fg C per bacteria (Cotner and Biddanda 2002). All phototrophy and phagotrophy data is available at http://rdi.uncoma.edu.ar/handle/uncomaid/16719.

The haptophyte *Chrysochromulina parva* is a small (< 5 µm) mixotrophic nanoflagellate that dominates nanoplankton in north Patagonian lakes (Modenutti et al. 2013; Queimaliños 2002). Phototrophy in C. *parva* (pg C cell^{-1} h^{-1}) was obtained from Callieri et al. (2007) in situ primary production estimates, performed in Andean mountain lakes at different depths in a light gradient (see Table 1 for irradiances). From this dataset, we selected the lakes in which *C. parva* represented more than 90% of the total phytoplanktonic cells > 2 µm (Table 1). On the other hand, C. *parva* phagotrophy (pg C cell^{-1} h^{-1}) was obtained from Balseiro et al. (2004) and Schenone et al. (2020) field bacterivory experiments performed in 5 Andean mountain lakes at different depths in a light gradient (see Table 1 for irradiances).

The mixotrophic ciliate *O. naumanni* is a peritrich that contains algae of the genus *Chlorella* (up to 450 cells per ciliate), and it is the most important and abundant mixotrophic ciliate in many north Patagonian Andean lakes (Modenutti et al. 2013). Phototrophy in *O. naumanni* (pg C ind^{-1} h^{-1}) was obtained from Modenutti et al. (2004) laboratory primary production determinations on *O. naumanni* in an experimental light gradient (Table 1). Laboratory experiments allow isolating *O. naumanni* primary production from other small primary producers. On the other hand, *O. naumanni* phagotrophy (pg C ind^{-1} h^{-1}) was obtained from Balseiro et al. (2004) and Modenutti and Balseiro (2020) field and laboratory bacterivory experiments using *O. naumanni* under different irradiances (Table 1).

Phototrophy and phagotrophy mechanistic models

Phototrophy (*P*) was modelled using Platt et al. (1980) formulation, which is a three-parameter non-monotonic equation for phototrophy as a function irradiance (*I*). This non-monotonic equation accounts for decreasing photosynthesis at high irradiances due to photoinhibition, conferring more flexibility to a wider irradiance range than monotonic hyperbolic formulations (Jassby and Platt 1976). Therefore, the non-monotonic Platt formulation has been preferred to model phototrophy in environments with high irradiance where photo-inhibition and light damage are relevant factors, such as the marine pelagic zone and oligotrophic mountain lakes (Forget et al. 2007).

$$P_{(I)} = P_{\max} \times \left(1 - e^{\frac{-\alpha \times I}{P_{\max}}}\right) \times e^{\frac{-\beta \times I}{P_{\max}}} \quad (1)$$

where P_{max} (pg C cell^{-1} h^{-1} in CM or pg C ind^{-1} h^{-1} in NCM) is the maximum theoretical phototrophy (i.e. the assimilation number in Platt formulation); α (pg C cell^{-1} h^{-1} µmol photon^{-1} m^2 s or pg C ind^{-1} h^{-1} µmol photon^{-1} m^2 s) is the phototrophy increasing slope at low irradiances; and β (pg C cell^{-1} h^{-1} µmol photon^{-1} m^2 s or pg C ind^{-1} h^{-1} µmol photon^{-1} m^2 s) is the phototrophy decreasing slope at high irradiances (Platt et al. 1980).

On the other hand, phagotrophy (B) by both mixotrophic protists was modelled as a function of prey abundance (*N*, ng C mL^{-1}) using Michaelis–Menten formulation (Eq. 2).

$$B_{(N)} = B_{\max} \times \frac{N}{k + N} \quad (2)$$

where B_{max} (pg C cell^{-1} h^{-1} in CM or pg C ind^{-1} h^{-1} in NCM) is the phagotrophy at prey saturation and *k* (ng C

mL^{-1}) is the prey concentration where predator saturation starts. Then, the maximum phagotrophy was modelled with a four-parameter non-monotonic equation based on Platt et al. (1980) formulation:

$$B_{\max(I)} = b_{\max} \times \left(1 - e^{\frac{-\left(\alpha' \times I + \gamma'\right)}{b_{\max}}}\right) \times e^{\frac{-\beta' \times I}{b_{\max}}} \quad (3)$$

where b_{max} (pg C $cell^{-1}$ h^{-1} in CM or ind^{-1} h^{-1} in NCM) is the maximum theoretical phagotrophy; α' (pg C $cell^{-1}$ h^{-1} µmol $photon^{-1}$ m^2 s or pg C ind^{-1} h^{-1} µmol $photon^{-1}$ m^2 s) is the phagotrophy increasing slope at low irradiances; and β' (pg C $cell^{-1}$ h^{-1} µmol $photon^{-1}$ m^2 s or pg C ind^{-1} h^{-1} µmol $photon^{-1}$ m^2 s) is the phagotrophy decreasing slope at high irradiances. In addition, γ' (pg C $cell^{-1}$ h^{-1} or ind^{-1} h^{-1}) is an extra parameter independent of irradiance which accounts for phagotrophy in darkness ($I = 0$):

$$B_{\max(I=0)} = b_{\max} \times \left(1 - e^{\left(\frac{-\gamma'}{b_{\max}}\right)}\right) \quad (4)$$

This term was added because phagotrophy is not 0 in darkness as it is phototrophy in Platt's equation. Therefore, our final phagotrophy model as a function of both prey abundance and irradiance (Eq. 5) is the joint of the Michaelis–Menten (Eq. 2) and our modified Platt formulations (Eq. 3):

$$B_{(N,I)} = b_{\max} \times \left(1 - e^{\frac{-(\alpha' \times I + \gamma')}{b_{\max}}}\right) \times e^{\frac{-\beta' \times I}{b_{\max}}} \times \frac{N}{k + N} \quad (5)$$

Model calibration and sensitivity analysis

The use of non-linear equations to represent ecological dynamics, such as trophic interactions, could lead to high computational costs for estimating parameters correctly (Clark 2005). In this context, Bayesian inference provides an excellent framework by combining the empirical data with prior information on the parameters (Arhonditsis et al. 2008). Bayesian analysis was performed using STAN code interfaced with R (R Core 2019) through the 'brms' package (Bürkner 2017). We fitted the Platt et al. (1980) model (Eq. 1 with three parameters: P_{max}, α and β) with *C. parva* and *O. naumanni* phototrophy data (84 and 32 data points, respectively). In addition, we fitted our phagotrophy model (Eq. 5 with five parameters: b_{max}, α', β', γ' and k) with *C. parva* and *O. naumanni* phagotrophy data (24 and 34 data points, respectively). We obtained four model fits hereafter named as 'CM-Phot', 'NCM-Phot', for phototrophy of *C. parva* and *O. naumanni,* respectively; and 'CM-Phag', and 'NCM-Phag', for phagotrophy of *C. parva* and *O. naumanni,* respectively. The effect of different sources of variation (field versus laboratory and among lakes) was quantified by applying a hierarchical Bayesian modelling approach. Hierarchical Bayesian models are particularly useful to include all the empirical data in a single analysis by allowing the information on one subsystem (e.g. an intensively sampled location) to be generalised to other subsystems (e.g. scantily sampled locations) through shared higher-level parameters (Clark 2005; Norros et al. 2017). We assumed parameter values for each subsystem (different lakes, or laboratory vs field conditions) as a sample from a shared lognormal distribution (Norros et al. 2017).

To assure that our model posteriors are governed by the experimental data and not by the priors, we performed a sensitivity analysis using four different sets of priors for the initial dynamics of model parameters, from highly informative to less informative based on the variance of their probability distributions (Table S1). In all cases, normal distributions with increasing variance were preferred over flat uniform distributions to avoid convergence problems (Bürkner 2017). Then, posterior mean and probability intervals of model parameters were calculated and compared by quantifying the overlap between them (Arhonditsis et al. 2008). Finally, we performed posterior predictive checks to our models fitted with the different set of priors and calculated the Bayesian R^2 for fit accuracy between the observed and predicted values (Bürkner 2017). Details on the statistical analysis and Bayesian methods are available in the R script available at http://rdi.uncoma.edu.ar/handle/uncomaid/16719 and in the supplementary material.

Model validation and predictive accuracy

We assessed the predictive accuracy of our mechanistic models with out-of-sample data (Boyce et al. 2002). Our out-of-sample assessment was based on a K-fold cross-validation approach that iteratively split our datasets into 90% training data and 10% test data withheld from model fitting. We repeated this procedure ten times ($K = 10$), with no test data repetition between folds (Wenger and Olden 2012). We then validated our models using mean absolute error (MAE) calculated for each of the ten folds test datasets. MAE can be interpreted on the data's original scale as the difference between observed and predicted phototrophy and phagotrophy rates. Model predictions for phototrophy and phagotrophy of both mixotrophic protists were estimated for an irradiance range of 0–2000 µmol photon m^{-2} s^{-1}. For phagotrophy, prey abundance was set in a range of $0.3–1.7 \times 10^6$ bacteria mL^{-1} which is equivalent to 5–25 ng C mL^{-1} assuming 15 fg per cell based on Cotner and Biddanda (2002).

Metrics for phototrophy and phagotrophy balance

To quantify and compare the balance between phototrophy and phagotrophy of mixotrophic protists estimated by our models, we analysed three metrics: the phototrophy and phagotrophy low and high light adaptation indexes; the relative phototrophy vs the relative phagotrophy; and the phototrophy:phagotrophy ratio as a function of light. Phototrophy low and high light adaptation indexes (I_α and I_β, respectively) were obtained following Platt et al. (1980) as the ratios between the posterior parameter distributions of Eq. 1:

$$I_\alpha = \frac{P_{\max}}{\alpha} \; and \; I_\beta = \frac{P_{\max}}{\beta}$$

These indexes indicate the irradiance (µmol photon m^{-2} s^{-1}) where saturation (i.e. maximum phototrophy) and photoinhibition starts, respectively. Likewise, phagotrophy low and high light adaptation indexes ($I_{\alpha'}$ and $I_{\beta'}$, respectively) were calculated using the posterior parameter distributions of Eq. 5:

$$I_{\alpha'} = \frac{b_{\max}}{\alpha'} \; and \; I_{\beta'} = \frac{b_{\max}}{\beta'}$$

These indexes are equivalent to those of phototrophy sharing the same irradiance units. Particularly, $I_{\alpha'}$ and $I_{\beta'}$ indicate the irradiance where saturation ($I_{\alpha'}$) and inhibition ($I_{\beta'}$) of phagotrophy begins.

The relative phototrophy and phagotrophy values (adimensional proportion ranging from 0 to 1) was normalized by their respective maximum values. Finally, the phototrophy:phagotrophy ratio (adimensional) was obtained by dividing the relative phototrophy with the relative phagotrophy along the light gradient. In these cases, prey abundance was fixed to 15 ng C mL^{-1}.

Results

Experimental data and model fit

We found a non-monotonic effect of irradiance on phototrophy of both *C. parva* and *O. naumanni* in the primary production experiments obtained from previous published works (Fig. 1 circles). In *C. parva* (CM), the highest phototrophy rates were observed at low to intermediate irradiance (20 to 300 µmol photon m^{-2} s^{-1}) while the lowest phototrophy rates were observed at high irradiance (> 1000 µmol photon m^{-2} s^{-1}). In *O. naumanni* (NCM), the highest phototrophy rates were also observed at low to intermediate irradiance (35 and 110 µmol photon m^{-2} s^{-1}) while lower values were found at higher irradiances (> 300 µmol photon m^{-2} s^{-1}). Accordingly, our models 'CM-Phot' and 'NCM-Phot' displayed non-monotonic functions with increasing irradiance in both CM and NCM phototrophy, respectively (Fig. 1 solid lines). Both models showed a good fit accuracy to the observed data ('CM-Phot' $R^2 = 0.72$ and 'NCM-Phot' $R^2 = 0.68$) as most points were located within the Bayesian 95% credible interval (Fig. 1 grey bands).

Phagotrophy was adjusted to the prey abundance and irradiances obtained from previous published works (Table 1). The effect of irradiance and prey abundance was analysed simultaneously with our phagotrophy models 'CM-Phag' and 'NCM-Phag', obtaining a tridimensional surface for each mixotroph (Fig. 2). We found a hyperbolic effect of prey abundance and a non-monotonic effect of irradiance on phagotrophy of both *C. parva* and *O. naumanni*. In *C. parva* (CM), the highest phagotrophy rates were observed at intermediate irradiance (100–300 µmol photon m^{-2} s^{-1}, Fig. 2 circles) and the lowest values were found at high irradiance (> 750 µmol photon m^{-2} s^{-1}). In *O. naumanni* (NCM), the highest phagotrophy was found at low irradiance (35 µmol photon m^{-2} s^{-1}, Fig. 2 circles) and lower values were found at higher irradiances (> 300 µmol photon m^{-2} s^{-1}). Both models showed a good fit accuracy to the observed data ('CM-Phag' $R^2 = 0.86$ and 'NCM-Phag' $R^2 = 0.71$).

Model validation and predictive accuracy

The sensitivity analysis on the priors distributions of the model parameters showed a high overlap between their posterior distributions, regardless of the selected priors (Figures S1, S2 and S3). All our mechanistic models showed an excellent predictive accuracy to the test datasets. The out-of-sample MAE for each of the tenfold validations in each model can be found in Table S2. Briefly, the mean between the MAE of the tenfold validations and the different sets of prior distributions were 0.08 and 0.07 pg C $cell^{-1}$ h^{-1} in the 'CM-Phot' and 'CM-Phag' models, respectively; and 26.4 and 1.7 pg C ind^{-1} h^{-1} in the 'NCM-Phot' and 'NCM-Phag' models, respectively. In most cases, these differences between observed and model predicted phototrophy and phagotrophy rates represented less than the 20% of the mean observed values at each irradiance level and were located within the Bayesian 95% credible interval (Table S2).

Metrics for phototrophy and phagotrophy balance

In Fig. 3, we compared mixotrophic functional types using the light adaptation indexes calculated from the posterior parameter distributions of phototrophy and phagotrophy models. In both mixotrophs, we found that the phototrophy low light adaptation index ($I_\alpha I_\alpha$) was lower than phagotrophy low light adaptation index ($I_{\alpha'} I_{\alpha'}$) (Fig. 3 a and c); and phototrophy high light adaptation index ($I_\beta I_\beta$) was higher

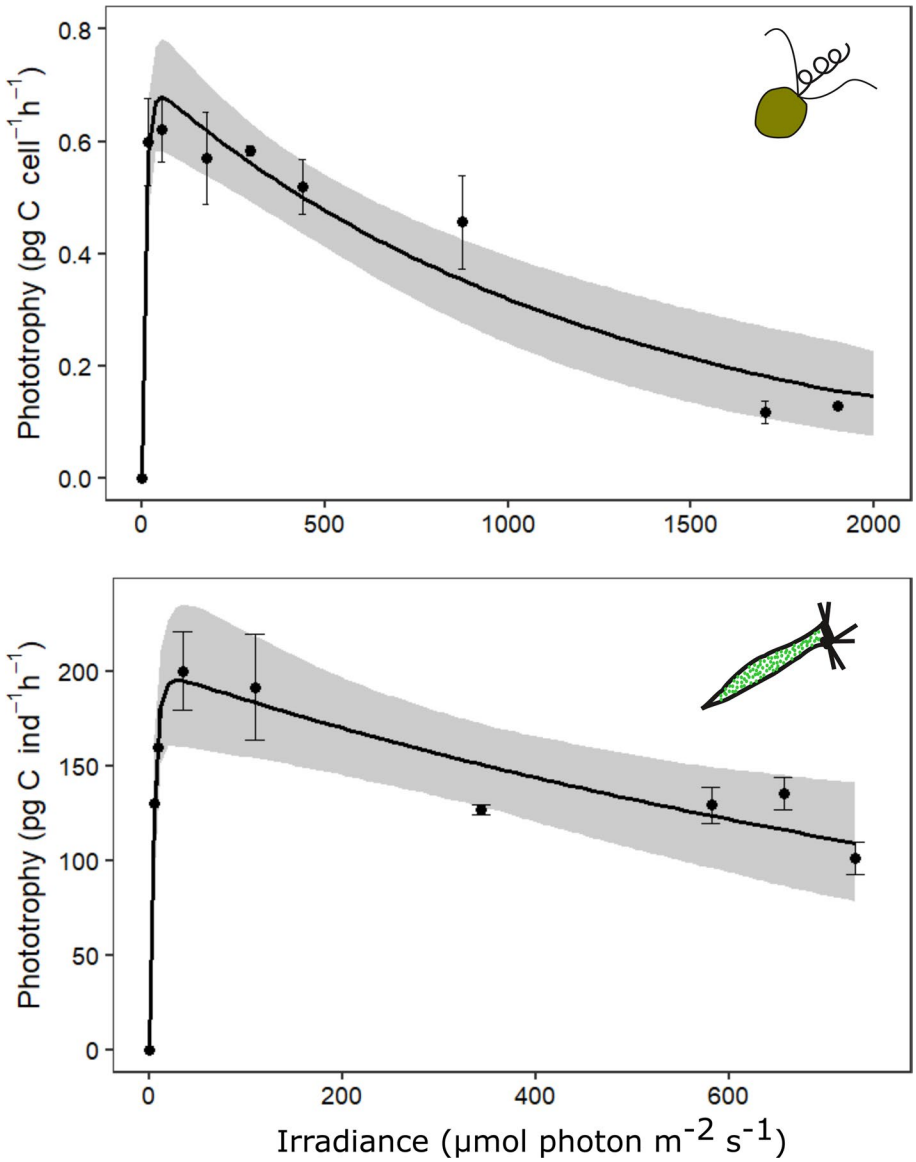

Fig. 1 *Chrysochromulina parva* (CM) and *Ophrydium naumanni* (NCM) phototrophy curves as a function of irradiance obtained from our models fitted with field and laboratory primary production experiments. Mean and standard errors of observed phototrophy rates are represented by the black circles and error bars (3–4 replicates per circle, $n = 84$ in CM and 24 in NCM). The solid line is the mean phototrophy estimated by the 'CM-Phot' and the 'NCM-Phot' models. Grey bands represent the Bayesian 95% credible intervals

than phagotrophy high light adaptation index ($I_{\beta'}I_{\beta'}$) (Fig. 3 b and d). However, the overlap between posterior distributions of these metrics was higher for *C. parva* (CM) than for *O. naumanni* (NCM). The percentage of overlap between phototrophy and phagotrophy low light indexes was 7.8% in *C. parva* and 0.4% in *O. naumanni*, while the percentage of overlap between phototrophy and phagotrophy high light indexes were 24.3% in *C. parva* and < 0.1% in *O. naumanni*.

In Fig. 4, we compared the relative phototrophy and phagotrophy within mixotrophic species. At irradiance zero (i.e. phototrophy = 0), the relative phagotrophy was three times higher in *C. parva* than in *O. naumanni* (0.51 and 0.17, respectively). Then, from low to intermediate irradiances (0–65 µmol photon m^{-2} s^{-1}, Fig. 4 red dots), relative phagotrophy increased more linearly with increasing phototrophy in *C. parv*a than in *O. naumanni*. Finally, from intermediate to high irradiance (65–325 and 325–2000 µmol photon m^{-2} s^{-1}, Fig. 4 green and blue dots, respectively), the decrease of relative phagotrophy with decreasing phototrophy was more linear in *C. parva* than in *O. naumanni*. At half maximum phototrophy (i.e. relative phototrophy = 0.5), the relative phagotrophy was ~ 0.47 in *C. parva* and ~ 0.14 in *O. naumanni*.

In Fig. 5, we compared the phototrophy:phagotrophy ratios between mixotrophic species for an irradiance range from 0 to 500 µmol photon m^{-2} s^{-1} and a fixed prey abundance of 15 ng C mL^{-1}. We found that *C. parva* (CM) ratio increased at very low irradiances (quick increase in phototrophy over phagotrophy) reaching values near 1 and then remained around this value from intermediate to high irradiances (Fig. 5 dotted line). On the contrary, the *O.*

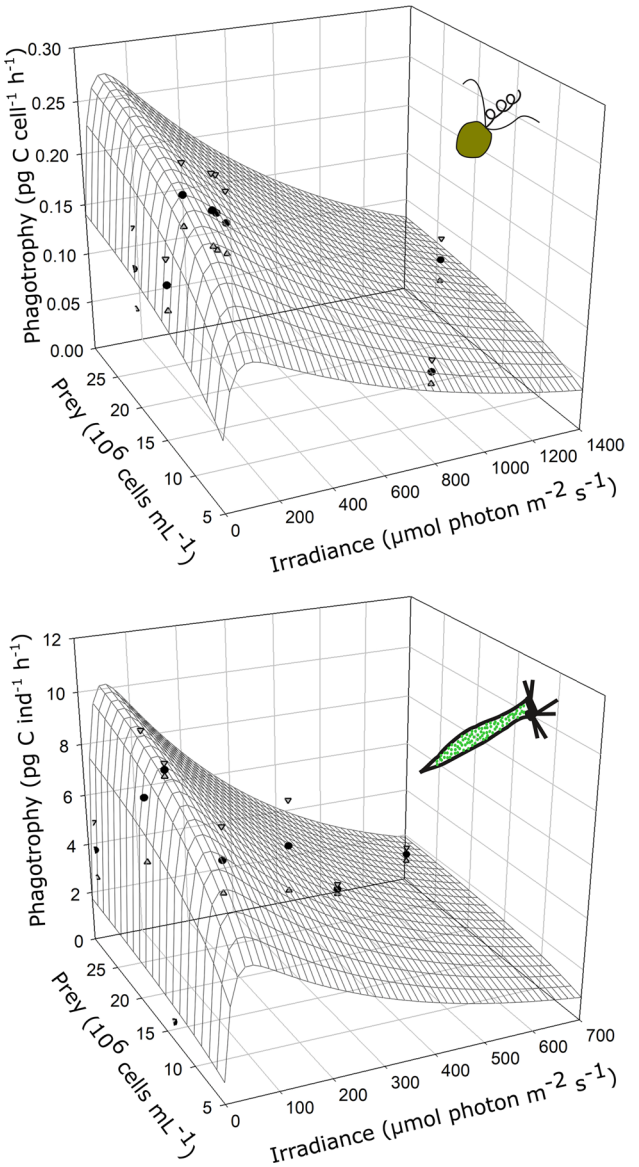

Fig. 2 *Chrysochromulina parva* (CM) and *Ophrydium naumanni* (NCM) phagotrophy 3D surfaces as a function of prey abundance and irradiance obtained from our models fitted with field and laboratory bacterivory experiments. Means of observed phagotrophy rates are represented by the black circles (3–4 replicates per circle, $n = 32$ in CM and 34 in NCM) and standard deviations are represented with the triangles. The 3D mesh is the mean phagotrophy estimated by the 'CM-Phag' and the 'NCM-Phag' models

naumanni (NCM) ratio showed a more complex pattern. At low irradiances the ratio increased rapidly, reaching values higher than 1.5, but decreasing to 1 at an irradiance range of 50–100 µmol photons m^{-2} s^{-1}. At these light intensities, both CM and NCM ratios were very similar and around 1. However, as the light increased beyond 100 µmol photons m^{-2} s^{-1}, the phototrophy:phagotrophy ratio of *O. naumanni* turned to a constant increase reaching values higher than 2 at the maximum irradiance tested (Fig. 5 solid line). Finally, the combined effect of prey abundance and irradiance on the phototrophy:phagotrophy ratio was assessed with a 3D plot (Figure S4).

Discussion

In this work, we found that irradiance has a non-monotonic effect on phototrophy and phagotrophy of both studied mixotrophic protists (*C. parva* and *O. naumanni*), meaning that both nutritional strategies increase when irradiance is low and decrease when irradiance is high. Moreover, our mechanistic models based on Platt's formulations and fitted with Bayesian methods successfully represented these functions and the cross-validation test showed good predictive accuracy. Platt's formulations (Platt et al. 1980) are particularly relevant for phototrophy in deep oligotrophic systems that develop a DCM, where the highest phototrophic plankton abundance and primary production occurs (Bouman et al. 2018; Forget et al. 2007). In these systems, being above or under the DCM implies a decrease in the phototrophic efficiency (Callieri et al. 2007; Modenutti et al. 2004). Accordingly, Platt et al. (1980) formulation highlights an optimal irradiance range where phototrophy is maximum. On the other hand, phagotrophy by mixotrophs showed a hyperbolic effect with prey abundance and a non-monotonic function with irradiance that overlaps the optimal irradiance range with that of phototrophy. Higher bacterivory rates also occur in the DCM where phototrophic picoplankton is more abundant (Modenutti and Balseiro 2002). Therefore, mixotrophic protists (*C. parva* and *O. naumanni*) from Andean freshwater oligotrophic systems are adapted to attain maximum feeding efficiency (both phototrophy and phagotrophy) at optimum irradiances (20–200 µmol photons m^{-2} s^{-1}), observed in the DCM.

Mixotrophic phototrophy and phagotrophy functions increase at low irradiances, indicating that both nutritional strategies benefit from increasing irradiance when limiting. According to our model results, the low light adaptation index was higher for phototrophy than phagotrophy in both *C. parva* and *O. naumanni*, suggesting that phototrophy is more flexible than phagotrophy at low irradiances (Platt et al. 1980). The main reason for this difference is that phototrophy is not possible at irradiance zero, while phagotrophy occurs (Jones 1997; McKie-Krisberg et al. 2015). Consequently, our phagotrophy model (Eq. 5) has an extra parameter (γ) in the Platt formulation (Eq. 1), which accounts for phagotrophy estimation at irradiance zero. This new parameter was relatively higher in *C. parva* than in *O. naumanni*, matching the experimentally obtained phagotrophy at irradiance near to zero. In addition, the high overlap

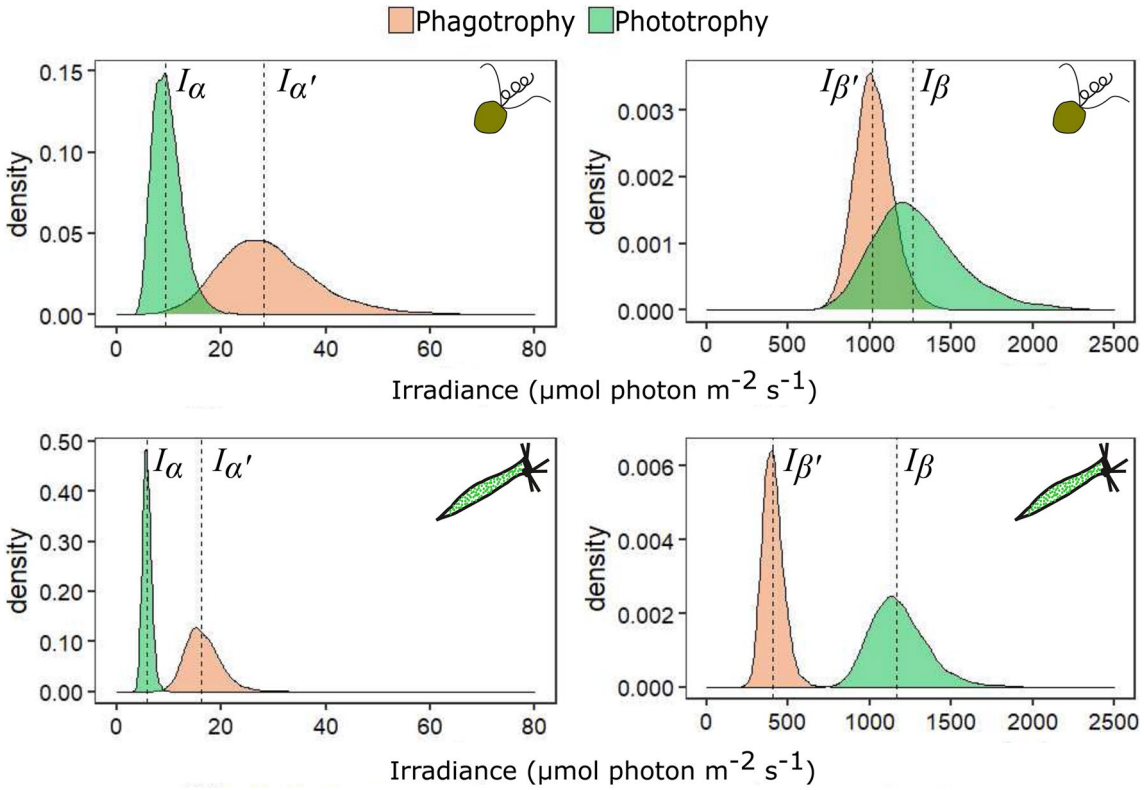

Fig. 3 Light adaptation indexes of the mixotrophic protists studied based on the posterior distributions of the phototrophy (green) and phagotrophy (red) models: low light (**a**, **c**) and high light (**b**, **d**) adaptation indexes, **a** and **b**: *Chrysochromulina parva* (CM), **c** and **d**: *Ophrydium naumanni* (NCM)

of the phototrophy and phagotrophy low light adaptation indexes found in *C. parva* show that these functions are more coupled in the nanoflagellate than in the mixotrophic ciliate and thus the phototrophy:phagotrophy balance is more variable in the latter at low irradiances.

The increasing trend in phototrophy and phagotrophy registered at low irradiances changes at intermediate and high ones where a decreasing trend is observed, suggesting that excessive irradiance impairs both nutritional strategies. The decrease in phototrophic efficiency due to photo-inhibition is well documented (Falkowski and Raven 2007; Kirk 1994; Platt et al. 1980). The light was also shown to affect bacterivory (Berge et al. 2017; Fischer et al. 2017) and more recently MNF phagotrophy was observed to decrease under high irradiances (Schenone et al. 2020). The output of our model showed that in the CM (*C. parva*), the high light adaptation indexes were similar between phototrophy and phagotrophy, but in the NCM (*O. naumanni*) these indexes were considerably different. The high light adaptation index indicates the irradiance where photoinhibition starts. In the case of *O. naumanni*, the phagotrophy high light adaptation index was considerably lower than the phototrophic one, meaning that at high irradiance, phagotrophy is significantly more affected than phototrophy in the mixotrophic ciliate. The cell of peritrich ciliates is highly contractile and shows extreme shape variation, depending on environmental conditions (Corliss 1979; Winkler and Corliss 1965). In particular, the length of an *O. naumanni* individual is highly variable, allowing the endosymbiotic *Chlorella* to be arranged to optimise the light received. At low irradiance, *O. naumanni* adopts an elongate form to maximise photosynthesis, but high irradiance causes cell contraction (Modenutti et al. 2004). During the cell contraction, peritrich zooids reduce ciliature beating and thus, the feeding current that moves food particles towards the cell (Ryu et al. 2017). Consequently, the mixotrophic ciliate would reduce phagotrophy in a more pronounced way than phototrophy as was obtained in the output of our model.

Novel planktonic food web models fitted with empirical data recognize mixotrophic protists as a diverse assemblage in terms of functional-allometric differences and contrasting nutritional strategies between CM and NCM (Caron 2016; Leles et al. 2021). The size of the CM in our study (the MNF *C. parva*) is comparable to that of endosymbiotic *Chlorella* cells in the mixotrophic ciliate. However, *O. naumanni* contains hundreds of cells in one individual (Modenutti et al. 2004; Queimaliños et al. 1999), and accordingly, the C fixation per individual is almost 300-fold that

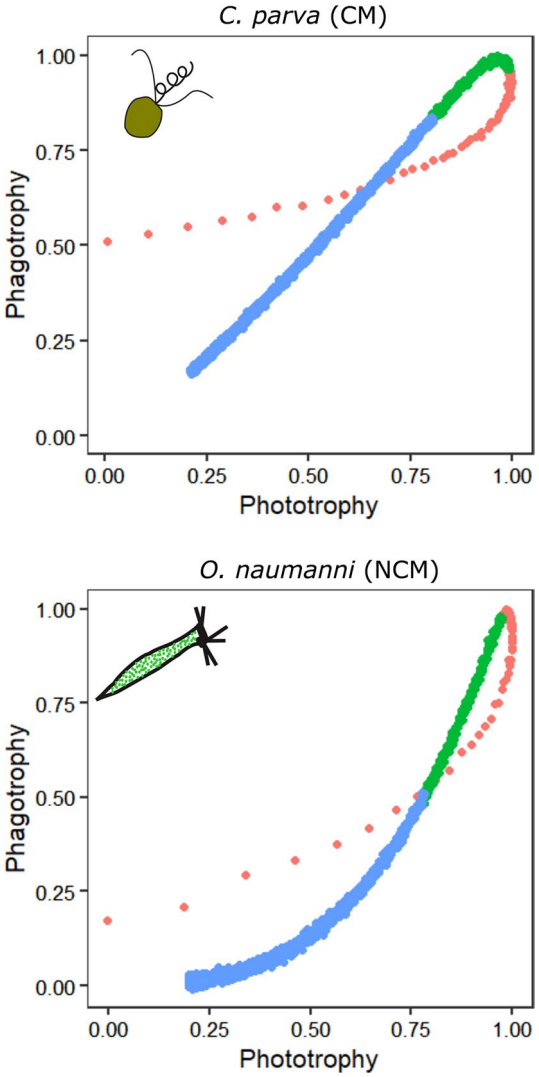

Fig. 4 Predicted relative phototrophy and phagotrophy (proportions obtained by dividing all values by its maximum) of *Chrysochromulina parva* (CM) and *Ophrydium naumanni* (NCM) for an irradiance range of 0–2000 µmol photon m^{-2} s^{-1} and prey abundance set to 15 ng C mL^{-1}. Red dots indicate low irradiances (< 65 µmol photon m^{-2} s^{-1}), while green and blue dots indicate intermediate and high irradiances (65–325 µmol photon m^{-2} s^{-1} and > 325 µmol photon m^{-2} s^{-1}, respectively)

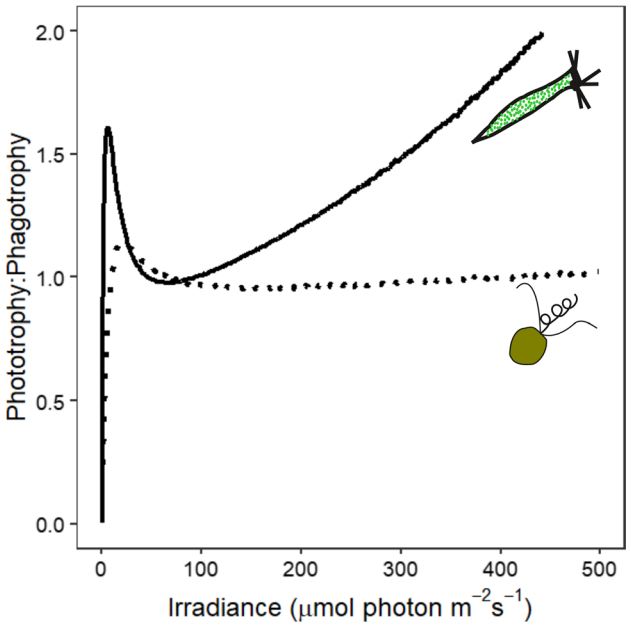

Fig. 5 The ratio between phototrophy and phagotrophy of *C. parva* (CM) (dotted line) and *O. naumanni* (NCM) (solid line) as a function of irradiance (proportions obtained by dividing all values by its maximum) predicted for an irradiance range of 0–2000 µmol photon m^{-2} s^{-1} and prey abundance set to 15 ng C mL^{-1}

of a *C. parva* cell. In addition, we found that the balance between phototrophy and phagotrophy is more constant in *C. parva* than *O. naumanni* throughout the light gradient, indicating that these nutritional strategies are more coupled in the former. For a CM, such as *C. parva*, both phototrophy and phagotrophy functions have co-evolved in the same cell (Troost et al. 2005), and thus can attain similar responses to changes in the light environment. On the other hand, mixotrophic ciliates are primarily phagotrophic, comprising a wide range of functional and numerical responses to prey and environmental conditions (Weisse 2017). Here, we found that changing the light environment (lower and higher irradiance than the optimal) has a strong negative effect by decoupling phagotrophy from phototrophy in *O. naumanni*. These results would explain the low performance and survival of this species in the epilimnetic zone (high irradiance) outside the DCM (Modenutti et al. 2008).

Light climate is one of the lake parameters with high susceptibility to change because of global changes such as glacial recession and land use (Bastidas Navarro et al. 2018; Kritzberg 2017; Rose et al. 2014). In this sense, our models predict a more constant phototrophy–phagotrophy balance in *C. parva* than in *O. naumanni* under extreme low or high light scenarios. Phagotrophy allows CMs to survive under prolonged dark periods in Antarctic lakes, and then supplies phototrophy when the light climate is optimal (Laybourn-Parry et al. 2005). Moreover, CMs dominate turbid proglacial lakes where minerogenic suspensoids affect phagotrophy through interference and by changing light penetration (Schenone et al. 2020). Temperature is another key variable affecting nutrition of mixotrophic protists (Princiotta et al. 2016; Wilken et al. 2013). Particularly, Wilken et al. (2013) showed experimentally that increasing water temperature reduces phototrophy and increases phagotrophy in the nanoflagellate *Ochromonas sp.* (CM), and that this decoupling is more pronounced with increasing irradiance from low to intermediate. Light also influences the uptake of other resources by mixotrophic protists, such as dissolved

nutrients and prey availability (Edwards 2019; Hansson et al. 2019). Dissolved nutrient uptake was observed to be direct in CM (i.e. osmotrophy) and indirect in the NCM by eating prey with different nutritional quality (Maselli et al. 2022; McKie-Krisberg et al. 2015; Schoener and McManus 2017). Moreover, the importance of phagotrophy over phototrophy and osmotrophy along the light gradient is highly diverse among mixotrophs (Jones 2000; Stoecker 1998) and within functional groups (Leles et al. 2018). Therefore, irradiance has a key role in determining the nutritional balance in mixotrophic protists, both directly and combined with other environmental variables sensitive to global change.

In this work, we present a general mechanistic model to consider phototrophy and phagotrophy by mixotrophic protists under different light scenarios. We calibrate this model (i.e. estimate its parameters) with two protists of different physiologies (CM and NCM) but corresponding to the type C in which phototrophy and phagotrophy changes proportionally with light (Jones 1997). However, the model has the potential to be calibrated with other ecological types of mixotrophs, such as Type B (Jones 1997), where phagotrophy decreases with increasing light (e.g. $\alpha' = 0$).

In conclusion, our modelling approach allowed us to compare mixotrophic protists (CM and NCM) by assessing quantitatively the balance between their nutritional strategies in the widest range of light scenarios. These different mixotrophic protists coexist in aquatic ecosystems, playing a key role as primary and secondary producers in plankton communities and the microbial loop (Flynn et al. 2019; Zubkov and Tarran 2008). In this sense, our proposed models clearly identified how the two studied mixotrophic protists balance their nutritional modes under different scenarios of prey and light availability. Furthermore, the model is potentially applicable to other oligotrophic systems with dominance of mixotrophic protists (e.g. marine pelagic systems) with important implications for carbon and nutrient fluxes.

Supplementary Information The online version contains supplementary material available at https://doi.org/10.1007/s00442-022-05226-4.

Acknowledgements LS is a CONICET fellowship and BM and EB are CONICET researchers. This work was supported by the Fondo Para la Investigación Científica y Tecnológica Argentina (FONCyT), PICT 2017-1940, PICT 2018-1563, PICT 2020-0383 and the National University of Comahue UNComahue B-236.

Author contribution statement LS, EB and BM: conceived the study, collected the experimental data and wrote the manuscript. LS: carried out the statistical analysis and developed the model. All authors contributed to the final version of the manuscript.

Funding Fondo para la Investigación Científica y Tecnológica,PICT 2017-1940,Esteban Balseiro,PICT 2018-1563,Beatriz Modenutti,2020-0383,Esteban Balseiro

Data availability All the collected data and code for statistical analysis is available at http://rdi.uncoma.edu.ar/handle/uncomaid/16719

Declarations

Conflict of interest The authors declare no conflict of interests.

Ethics approval Not applicable.

Consent to participate Not applicable.

Consent to publication Not applicable.

References

Arhonditsis GB, Papantou D, Zhang W, Perhar G, Massos E, Shi M (2008) Bayesian calibration of mechanistic aquatic biogeochemical models and benefits for environmental management. J Mar Syst 73:8–30. https://doi.org/10.1016/j.jmarsys.2007.07.004

Azam F, Fenchel T, Field JG, Gray J, Meyer-Reil L, Thingstad F (1983) The ecological role of water-column microbes in the sea. Mar Ecol Prog Ser 10:257–263

Balseiro EG, Queimaliños CP, Modenutti BE (2004) Grazing impact on autotrophic picoplankton in two south Andean lakes (Patagonia, Argentina) with different light: nutrient ratios. Rev Chil Hist Nat 77:73–85. https://doi.org/10.4067/S0716-078X2004000100007

Bastidas Navarro M, Martyniuk N, Balseiro E, Modenutti B (2018) Effect of glacial lake outburst floods on the light climate in an Andean Patagonian lake: implications for planktonic phototrophs. Hydrobiologia 816:39–48. https://doi.org/10.1007/s10750-016-3080-4

Berge T, Chakraborty S, Hansen PJ, Andersen KH (2017) Modeling succession of key resource-harvesting traits of mixotrophic plankton. ISME J 11:212. https://doi.org/10.1038/ismej.2016.92

Bouman HA et al (2018) Photosynthesis–irradiance parameters of marine phytoplankton: synthesis of a global data set. Earth Syst Sci Data 10:251–266. https://doi.org/10.5194/essd-10-251-2018

Boyce MS, Vernier PR, Nielsen SE, Schmiegelow FK (2002) Evaluating resource selection functions. Ecol Model 157:281–300. https://doi.org/10.1016/S0304-3800(02)00200-4

Bürkner P-C (2017) brms: an R package for Bayesian multilevel models using Stan. J Stat Softw 80:1–28. https://doi.org/10.18637/jss.v080.i01

Callieri C, Modenutti B, Queimalinos C, Bertoni R, Balseiro E (2007) Production and biomass of picophytoplankton and larger autotrophs in Andean ultraoligotrophic lakes: differences in light harvesting efficiency in deep layers. Aquat Ecol 41:511–523. https://doi.org/10.1007/s10452-007-9125-z

Caron DA (2016) Mixotrophy stirs up our understanding of marine food webs. PNAS 113:2806–2808. https://doi.org/10.1073/pnas.1600718113

Clark JS (2005) Why environmental scientists are becoming Bayesians. Ecol Lett 8:2–14. https://doi.org/10.1111/j.1461-0248.2004.00702.x

Corliss J (1979) Characterization, classification and guide to the literature. Pergamon Press, Oxford

Cotner JB, Biddanda BA (2002) Small players, large role: microbial influence on biogeochemical processes in pelagic aquatic ecosystems. Ecosystems 5:105–121. https://doi.org/10.1007/s10021-001-0059-3

Danger M, Leflaive J, Oumarou C, Ten-Hage L, Lacroix G (2007) Control of phytoplankton–bacteria interactions by stoichiometric constraints. Oikos 116:1079–1086. https://doi.org/10.1111/j.0030-1299.2007.15424.x

Edwards KF (2019) Mixotrophy in nanoflagellates across environmental gradients in the ocean. PNAS 116:6211–6220. https://doi.org/10.1073/pnas.1814860116

Falkowski PG, Raven JA (2007) Aquatic photosynthesis. Blackwell Science, Malden, MA USA

Fischer R, Giebel HA, Hillebrand H, Ptacnik R (2017) Importance of mixotrophic bacterivory can be predicted by light and loss rates. Oikos 126:713–722. https://doi.org/10.1111/oik.03539

Flynn KJ et al (2019) Mixotrophic protists and a new paradigm for marine ecology: where does plankton research go now? J Plankton Res 41:375–391. https://doi.org/10.1093/plankt/fbz026

Forget M-H et al (2007) Extraction of photosynthesis-irradiance parameters from phytoplankton production data: demonstration in various aquatic systems. J Plankton Res 29:249–262. https://doi.org/10.1093/plankt/fbm012

Hansson TH, Grossart HP, del Giorgio PA, St-Gelais NF, Beisner BE (2019) Environmental drivers of mixotrophs in boreal lakes. Limnol Oceanogr 64:1688–1705. https://doi.org/10.1002/lno.11144

Jassby AD, Platt T (1976) Mathematical formulation of the relationship between photosynthesis and light for phytoplankton. Limnol Oceanogr 21:540–547. https://doi.org/10.4319/lo.1976.21.4.0540

Jones H (1997) A classification of mixotrophic protists based on their behaviour. Freshwat Biol 37:35–43. https://doi.org/10.1046/j.1365-2427.1997.00138.x

Jones RI (2000) Mixotrophy in planktonic protists: an overview. Freshwat Biol 45:219–226. https://doi.org/10.1046/j.1365-2427.2000.00672.x

Kirk JT (1994) Light and photosynthesis in aquatic ecosystems. Cambridge University Press, Cambridge

Kritzberg ES (2017) Centennial-long trends of lake browning show major effect of afforestation. Limnol Oceanogr Letters 2:105–112. https://doi.org/10.1002/lol2.10041

Laybourn-Parry J, Marshall WA, Marchant HJ (2005) Flagellate nutritional versatility as a key to survival in two contrasting Antarctic saline lakes. Freshwat Biol 50:830–838. https://doi.org/10.1111/j.1365-2427.2005.01369.x

Leles SG, Bruggeman J, Polimene L, Blackford J, Flynn KJ, Mitra A (2021) Differences in physiology explain succession of mixoplankton functional types and affect carbon fluxes in temperate seas. Prog Oceanogr 190:102481. https://doi.org/10.1016/j.pocean.2020.102481

Leles SG et al (2018) Modelling mixotrophic functional diversity and implications for ecosystem function. J Plankton Res 40:627–642. https://doi.org/10.1093/plankt/fby044

Maselli M, Van de Waal DB, Hansen PJ (2022) Impacts of inorganic nutrients on the physiology of a mixoplanktonic ciliate and its cryptophyte prey. Oecologia. https://doi.org/10.1007/s00442-022-05162-3

McKie-Krisberg ZM, Gast RJ, Sanders RW (2015) Physiological responses of three species of Antarctic mixotrophic phytoflagellates to changes in light and dissolved nutrients. Microb Ecol 70:21–29. https://doi.org/10.1007/s00248-014-0543-x

Mitra A et al (2014) The role of mixotrophic protists in the biological carbon pump. Biogeosciences 11:995–1005. https://doi.org/10.5194/bg-11-995-2014

Mitra A et al (2016) Defining planktonic protist functional groups on mechanisms for energy and nutrient acquisition: incorporation of diverse mixotrophic strategies. Protist 167:106–120. https://doi.org/10.1016/j.protis.2016.01.003

Modenutti B, Balseiro E (2020) Mixotrophic ciliates in North-Patagonian Andean lakes: stoichiometric balances in nutrient limited environments. Limnetica 39:263–274. https://doi.org/10.23818/limn.39.17

Modenutti B, Balseiro E, Callieri C, Queimaliños C, Bertoni R (2004) Increase in photosynthetic efficiency as a strategy of planktonic organisms exploiting deep lake layers. Freshwat Biol 49:160–169. https://doi.org/10.1046/j.1365-2427.2003.01169.x

Modenutti BE, Balseiro EG (2002) Mixotrophic ciliates in an Andean lake: dependence on light and prey of an *Ophrydium naumanni* population. Freshwat Biol 47:121–128. https://doi.org/10.1046/j.1365-2427.2002.00783.x

Modenutti BE, Balseiro EG, Bastidas Navarro M, Laspoumaderes C, Souza MS, Cuassolo F (2013) Environmental changes affecting light climate in oligotrophic mountain lakes: the deep chlorophyll maxima as a sensitive variable. Aquat Sci 75:361–371. https://doi.org/10.1007/s00027-012-0282-3

Modenutti BE, Balseiro EG, Callieri C, Bertoni R (2008) Light versus food supply as factors modulating niche partitioning in two pelagic mixotrophic ciliates. Limnol Oceanogr 53:446–455. https://doi.org/10.4319/lo.2008.53.2.0446

Nielsen ES (1952) The use of radio-active carbon (C14) for measuring organic production in the sea. ICES J Mar Sci 18:117–140. https://doi.org/10.1093/icesjms/18.2.117

Norros V, Laine M, Lignell R, Thingstad F (2017) Parameterization of aquatic ecosystem functioning and its natural variation: Hierarchical Bayesian modelling of plankton food web dynamics. J Mar Syst 174:40–53. https://doi.org/10.1016/j.jmarsys.2017.05.004

Nygaard K, Tobiesen A (1993) Bacterivory in algae: a survival strategy during nutrient limitation. Limnol Oceanogr 38:273–279. https://doi.org/10.4319/lo.1993.38.2.0273

Platt T, Gallegos C, Harrison WG (1980) Photoinhibition of photosynthesis in natural assemblages of marine phytoplankton. J Mar Res 38:687–701

Princiotta SD, Smith BT, Sanders RW (2016) Temperature-dependent phagotrophy and phototrophy in a mixotrophic chrysophyte. J Phycol 52:432–440. https://doi.org/10.1111/jpy.12405

Ptacnik R, Sommer U, Hansen T, Martens V (2004) Effects of microzooplankton and mixotrophy in an experimental planktonic food web. Limnol Oceanogr 49:1435–1445. https://doi.org/10.4319/lo.2004.49.4_part_2.1435

Queimaliños C (2002) The role of phytoplanktonic size fractions in the microbial food webs in two north Patagonian lakes (Argentina). Intern Ver Für Theor Und Angew Limnol Ver 28:1236–1240

Queimaliños CP, Modenutti BE, Balseiro EG (1999) Symbiotic association of the ciliate Ophrydium naumanni with Chlorella causing a deep chlorophyll a maximum in an oligotrophic South Andes lake. J Plankton Res. https://doi.org/10.1093/plankt/21.1.167

R Core T (2019) R: A language and environment for statistical computing. R Foundation for Statistical Computing, Vienna, Austria. URL https://www.R-project.org/

Rose KC et al (2014) Light attenuation characteristics of glacially-fed lakes. J Geophys Res Biogeosci 119:1446–1457. https://doi.org/10.1002/2014JG002674

Ryu S, Pepper RE, Nagai M, France DC (2017) Vorticella: a protozoan for bio-inspired engineering. Micromachines 8:4. https://doi.org/10.3390/mi8010004

Schenone L, Balseiro EG, Bastidas Navarro M, Modenutti BE (2020) Modelling the consequence of glacier retreat on mixotrophic nanoflagellate bacterivory: a Bayesian approach. Oikos 129:1216–1228. https://doi.org/10.1111/oik.07170

Schoener DM, McManus GB (2017) Growth, grazing, and inorganic C and N uptake in a mixotrophic and a heterotrophic ciliate. J Plankton Res 39:379–391. https://doi.org/10.1093/plankt/fbx014

Sherr BF, Sherr EB, Fallon RD (1987) Use of monodispersed, fluorescently labeled bacteria to estimate in situ protozoan bacterivory. Appl Environ Microbiol 53:958–965. https://doi.org/10.1128/aem.53.5.958-965.1987

Stoecker DK (1998) Conceptual models of mixotrophy in planktonic protists and some ecological and evolutionary implications. Eur J Protistol 34:281–290. https://doi.org/10.1016/S0932-4739(98)80055-2

Stoecker DK, Johnson MD, de Vargas C, Not F (2009) Acquired phototrophy in aquatic protists. Aquat Microb Ecol 57:279–310. https://doi.org/10.3354/ame01340

Troost TA, Kooi BW, Kooijman SA (2005) Ecological specialization of mixotrophic plankton in a mixed water column. Am Nat 166:E45–E61. https://doi.org/10.1086/432038

Unrein F, Gasol JM, Not F, Forn I, Massana R (2014) Mixotrophic haptophytes are key bacterial grazers in oligotrophic coastal waters. ISME J 8:164. https://doi.org/10.1038/ismej.2013.132

Waibel A, Peter H, Sommaruga R (2019) Importance of mixotrophic flagellates during the ice-free season in lakes located along an elevational gradient. Aquat Sci 81:45. https://doi.org/10.1007/s00027-019-0643-2

Ward BA, Follows MJ (2016) Marine mixotrophy increases trophic transfer efficiency, mean organism size, and vertical carbon flux. PNAS 113:2958–2963. https://doi.org/10.1073/pnas.1517118113

Weisse T (2017) Functional diversity of aquatic ciliates. Eur J Protistol 61:331–358. https://doi.org/10.1016/j.ejop.2017.04.001

Wenger SJ, Olden JD (2012) Assessing transferability of ecological models: an underappreciated aspect of statistical validation. Methods Ecol Evol 3:260–267. https://doi.org/10.1111/j.2041-210X.2011.00170.x

Wilken S, Huisman J, Naus-Wiezer S, Van Donk E (2013) Mixotrophic organisms become more heterotrophic with rising temperature. Ecol Lett 16:225–233. https://doi.org/10.1111/ele.12033

Winkler RH, Corliss JO (1965) Notes on the rarely described, green colonial protozoon Ophrydium versatile (OFM) (Ciliophora, Peritrichida). Trans Am Microsc Soc 84:127–137

Yvon-Durocher G, Schaum C-E, Trimmer M (2017) The temperature dependence of phytoplankton stoichiometry: investigating the roles of species sorting and local adaptation. Front Microbiol 8:2003. https://doi.org/10.3389/fmicb.2017.02003

Zubkov MV, Tarran GA (2008) High bacterivory by the smallest phytoplankton in the North Atlantic Ocean. Nature 455:224. https://doi.org/10.1038/nature07236